THE JOURNAL OF BIOLOGICAL CHEMISTRY VOL. 289, NO. 19, pp. 13680–13690, May 9, 2014

Alternative Splicing Governs Cone Cyclic Nucleotide-gated (CNG) Channel Sensitivity to Regulation by Phosphoinositides*

Received for publication, February 28, 2014, and in revised form, March 22, 2014 Published, JBC Papers in Press, March 27, 2014, DOI 10.1074/jbc.M114.562272

Gucan Dai[‡§], **Tshering Sherpa**[§], **and Michael D. Varnum**[‡§¶1]

From the [§]*Department of Integrative Physiology and Neuroscience,* [‡]*Program in Neuroscience, and* [¶]*Center for Integrated Biotechnology, Washington State University, Pullman, Washington 99164-7620*

Background: Variants of photoreceptor CNG channels are produced by alternative splicing of precursor mRNA.
Results: Inclusion of an optional exon in human *CNGA3* transcripts produces channel isoforms with enhanced sensitivity to phosphoinositides via an allosteric mechanism.
Conclusion: Alternative splicing of *CNGA3* transcripts controls phosphoinositide regulation of cone CNG channels.
Significance: These findings reveal the functional importance of *CNGA3* alternative splicing.

Precursor mRNA encoding CNGA3 subunits of cone photoreceptor cyclic nucleotide-gated (CNG) channels undergoes alternative splicing, generating isoforms differing in the N-terminal cytoplasmic region of the protein. In humans, four variants arise from alternative splicing, but the functional significance of these changes has been a persistent mystery. Heterologous expression of the four possible CNGA3 isoforms alone or with CNGB3 subunits did not reveal significant differences in basic channel properties. However, inclusion of optional exon 3, with or without optional exon 5, produced heteromeric CNGA3 + CNGB3 channels exhibiting an ~2-fold greater shift in $K_{1/2,cGMP}$ after phosphatidylinositol 4,5-biphosphate or phosphatidylinositol 3,4,5-trisphosphate application compared with channels lacking the sequence encoded by exon 3. We have previously identified two structural features within CNGA3 that support phosphoinositides (PIP_n) regulation of cone CNG channels: N- and C-terminal regulatory modules. Specific mutations within these regions eliminated PIP_n sensitivity of CNGA3 + CNGB3 channels. The exon 3 variant enhanced the component of PIP_n regulation that depends on the C-terminal region rather than the nearby N-terminal region, consistent with an allosteric effect on PIP_n sensitivity because of altered N-C coupling. Alternative splicing of *CNGA3* occurs in multiple species, although the exact variants are not conserved across *CNGA3* orthologs. Optional exon 3 appears to be unique to humans, even compared with other primates. In parallel, we found that a specific splice variant of canine *CNGA3* removes a region of the protein that is necessary for high sensitivity to PIP_n. *CNGA3* alternative splicing may have evolved, in part, to tune the interactions between cone CNG channels and membrane-bound phosphoinositides.

Vertebrate visual transduction requires the activity of cyclic nucleotide-gated (CNG)[2] channels. Photoreceptor light responses generate a decrease in cGMP concentration that is converted into an electrical signal (membrane hyperpolarization) by the closure of CNG channels, leading to decreased neurotransmitter release onto second-order cells (1). Photoreceptor CNG channels are members of the large superfamily of cation-selective, "pore-loop" channels (2, 3). They are tetrameric proteins, with each subunit possessing six transmembrane segments, amino-terminal (N) and carboxyl-terminal (C) cytoplasmic domains, a central pore element contributing to the ion conduction pathway, and a cyclic nucleotide-binding domain located in the C-terminal region (4). Channel sensitivity to cGMP is tuned by several pathways, including the action of calcium sensor proteins such as calmodulin (5–9), serine/threonine and tyrosine phosphorylation (10, 11), extracellular matrix metalloproteinases (12, 13), and changes in the concentration of plasma membrane phosphoinositides such as PIP_2 and PIP_3 (14–16). Adjustments of CNG channel ligand affinity can contribute to photoreceptor adaptation and to paracrine and/or circadian changes in photoreceptor sensitivity (17–19).

The functional diversity of CNG channels is generated via several fundamental mechanisms. First, multiple genes encode CNG channel subunits, and cell type-specific expression of combinations of CNG channel subunits produce heteromeric channel assemblies having properties optimized for the role they play in those cells (4). For example, in cone and rod photoreceptors, the channels are composed CNGA3 and CNGB3 subunits or CNGA1 and CNGB1 subunits, respectively. Second, protein variants of CNGB1 (20, 21) and CNGA3 (22–24) are known to arise from alternative splicing of precursor mRNAs. Alternative splicing of primary transcripts is a prevalent mechanism for generating proteome complexity from a limited number of genes and is thought to have particular importance in the central nervous system (25). For CNGB1, a short variant (CNGB1b) is expressed in olfactory receptor neu-

* This work was supported by NEI, National Institutes of Health grant EY12836 (to M. D. V.).

[1] To whom correspondence should be addressed: Dept. of Integrative Physiology and Neuroscience, Washington State University, Box 647620, Pullman, WA 99164-7620. Tel.: 509-335-0661; Fax: 509-335-4650; E-mail: varnum@wsu.edu.

[2] The abbreviations used are: CNG, cyclic nucleotide-gated; PIP_2, phosphatidylinositol 4,5-biphosphate; PIP_3, phosphatidylinositol 3,4,5-trisphosphate; CaM, calmodulin; PIP_n, phosphoinositide(s).

rons where it forms part of the olfactory CNG channel, whereas a long variant (CNGB1a) is expressed in rod photoreceptor cells. In addition, the *CNGB1* transcriptional unit generates splice variants encoding soluble GARP1 and GARP2 proteins, short isoforms lacking the channel-forming domain but serving structural and regulatory functions. Soluble GARP proteins and the GARP region of CNGB1a are thought to interact with proteins in the rim of outer segment disc membranes, including phosphodiesterase (26) and peripherin (27). Furthermore, soluble GARP2 and the GARP region intrinsic to CNGB1a can act as gating inhibitors of the rod CNG channel (28). For human CNGA3, four protein isoforms can arise from alternative splicing because of different exon combinations within the 5′ region of the mRNA encoding the N-terminal cytoplasmic domain of the subunit (24, 29). Alternative splicing of *CNGA3* occurs in multiple species with many species-specific variants, including, in some cases, unique alternative cassette exons (22–24). Unlike *CNGB1*, the functional importance of *CNGA3* alternative splicing has remained an unresolved issue.

For many CNG channel subunits, the cytoplasmic N-terminal region can critically influence channel regulation by second messengers such as Ca^{2+}/CaM and phosphoinositides (9, 15, 16, 30–32). Previous studies in our laboratory have revealed two PIP_n regulation modules within CNGA3 subunits. One is located within the N-terminal region, overlapping with a functionally silent Ca^{2+}-CaM binding site, and the other is located within the C-terminal leucine zipper domain distal to the cyclic nucleotide-binding domain (16). Both of these PIP_n regulation modules are characterized by clusters of positively charged amino acids. Because alternative splicing produces changes in the N-terminal region of CNGA3, we hypothesized that these CNGA3 variants would exhibit altered channel sensitivity to regulation by PIP_n. Here we show that heteromeric channels formed with CNGA3 subunits having an optional e3 exon-encoded sequence exhibit enhanced sensitivity to regulation by phosphoinositides. Surprisingly, this enhancement of regulation depended on the PIP_n regulation module located in the C-terminal region of CNGA3, suggesting that changes in inter-domain N-C coupling may influence channel gating and regulation.

EXPERIMENTAL PROCEDURES

Channel Subunit cDNA and Mutagenesis—Human CNGA3 was a gift from Dr. K.-W. Yau (Johns Hopkins University, Baltimore, MD). Subunit cDNAs were subcloned into pGEMHE, where they are flanked by the *Xenopus* β-globin gene 5′- and 3′ UTRs for heterologous expression in *Xenopus* oocytes. Point mutations were generated by overlapping PCR (cassette) mutagenesis. All mutations were confirmed by fluorescence-based DNA sequencing.

Quantitative PCR—Human eyes were obtained from donors through SightLife with the approval of the Institutional Review Board at Washington State University. The eyes were immersed in RNAlater immediately after extraction. The retinas were subsequently isolated for RNA extraction. Retinal tissues, including the macula, were homogenized, and RNA extraction was performed (RNeasy mini kit, Qiagen, Valencia, CA), followed by on-column DNase treatment. The quantity of RNA was determined spectrophotometrically by the A_{260}/A_{280} ratio (Nanodrop 1000, Thermo-Scientific, Wilmington, DE).

Standard PCR was performed on all four variants of CNGA3 plasmid cDNA and on human retinal cDNA using JumpStart REDTaq ReadyMix (Sigma-Aldrich, St. Louis, MO). The primers used to detect the presence or absence of specific exons were as follows. For inclusion of exon 3, ATC GCC AGG TTT GGA AGA AT (forward) and CAT CCT CAG CAC ACC ACT GT (reverse); for skipping of exon 3, GAG ACC AGA GGA CTG GCT (forward) and GGC GCG ACA GCC TGG CGA (reverse); for inclusion of exon 5, AGG GAC CGG ACT CTT TTC CT (forward) and GGG CCA GGC GCT TCT CCC TC (reverse); for skipping of exon 5, GCA GAC AGA GGG AGA AGG AA (forward) and AAG ACA GGC AGG GCG ATG (reverse); and for constitutive exon 8, GTC CTG TAT GTC TTG GAT GTG C (forward) and CGT CTT GTA ATG CTG CCA CA (reverse). All primers were designed using Primer Express 3.0 (Applied Biosystems). The following conditions were used: initial denaturation, 94 °C (2 min); denaturation, 94 °C (30 s); annealing, 66 °C (30 s); extension, 72° (2 min); and final extension, 72 °C (5 min). 21 cycles for plasmid cDNAs and 39 cycles for human retinal cDNA were used.

Expression levels for inclusion of alternative exons in human retinal tissue were quantified by RT quantitative PCR. For each human retinal sample, first-strand cDNA was synthesized with 500 ng of total RNA, 100 ng of random primers (Invitrogen), and 50 units of reverse transcriptase (Superscript II, Invitrogen) according to the protocol of the manufacturer. RT quantitative PCR was performed using an iCycler version 2.039 thermocycler (Bio-Rad) according to the protocol of the manufacturer. The specificity of the reactions was verified via melt curve analysis. Three biological replicates and three technical replicates were performed for each sample. cDNA corresponding to constitutive exon 8 was used as an endogenous control. Before statistical analysis, Ct values were averaged across technical replicates.

Immunohistochemistry—Human retinal sections were purchased from Abcam (Cambridge, MA). Polyclonal goat anti-CNGA3 (1:500) was from Santa Cruz Biotechnology (catalog no. sc-21927, Dallas, TX). Rabbit polyclonal antibody specific to the exon 3-encoded sequence (1:300) was generated using the following peptide antigen: RFGRIQKKSQPEKV-[C] (GenScript, Piscataway, NJ). Fluorescein isothiocyanate-coupled peanut agglutinin (1:1000), which labels cone outer segments (33), was purchased from Sigma-Aldrich. Four slides, each containing two human retinal sections, were stained. The images were captured using a Leica TCS SP8 X point-scanning confocal microscope (Leica Microsystems, Buffalo Grove, IL).

PIP_2- and PIP_3-binding Assays—Purified GST fusion proteins were used for *in vitro* PIP_2- and PIP_3-binding assays in buffer containing 10 mM HEPES (pH 7.4), 50 mM NaCl, 2 mM EDTA, 0.25% v/v Triton X-100, and 0.25% v/v Nonidet P-40. PIP_2- and PIP_3-agarose beads were from Echelon Biosciences (Salt Lake City, UT). Briefly, 40 μl of a 50% slurry of PIP_n or control agarose beads and purified protein (2 μg/ml) was incubated in 0.5 ml of binding buffer for 2 h at 4 °C with rocking. Beads were pelleted gently and washed five times with excess binding buffer. PIP_n-interacting proteins were eluted with 1×

NuPAGE sample buffer (Invitrogen). Protein samples were then separated under reducing conditions in 4–12% BisTris gels and blotted onto nitrocellulose by using the NuPAGE transfer buffer system (Invitrogen). Blotted proteins were detected overnight using B-14 anti-GST monoclonal antibody (Santa Cruz Biotechnology) at a dilution of 1:2000 in 1% milk, 500 mM NaCl, 20 mM Tris-HCl (pH 7.5), and 0.05% Tween 20. Horseradish peroxide-conjugated anti-mouse IgG secondary antibodies were used subsequently for 1 h. Chemiluminescent detection was performed using the Super-Signal West Dura extended duration detection kit (Pierce).

Electrophysiology—For expression in *Xenopus laevis* oocytes, channel subunit cDNAs were linearized by digestion with NheI or SphI, and cRNA was synthesized *in vitro* using an upstream T-7 promoter (mMessage mMachine, Ambion). Stage IV oocytes were isolated as described previously (34). The animal use protocols were consistent with the recommendations of the American Veterinary Medical Association and were approved by the Institutional Animal Care and Use Committee of Washington State University. Approximately 20 ng of channel RNA was microinjected per oocyte. To efficiently generate heteromeric channels, an excess of CNGB3 relative to the CNGA3 subunit RNA was injected (35). 2–7 days after microinjection of *in vitro*-transcribed cRNA into oocytes, patch clamp experiments were performed using an Axopatch 200B amplifier (Axon Instruments, Foster City, CA) and pulse acquisition software (HEKA, Bellmore, NY) in the inside-out configuration. Initial pipette resistances were 0.30–0.80 MΩ. Intracellular (bath) and extracellular (pipette) solutions contained 130 mM NaCl, 0.2 mM EDTA, and 3 mM HEPES (pH 7.2). Cyclic nucleotides were added to the intracellular solution as needed. Intracellular solutions were changed using an RSC-160 rapid solution changer (Molecular Kinetics, Indianapolis, IN). Currents in the absence of cyclic nucleotide were subtracted. For channel activation by cGMP, dose-response data were fitted using the Hill equation, $I / I_{max} = [cGMP]^h / ({K_{1/2}}^h + [cGMP]^h)$, where I is the current amplitude at +80 mV, I_{max} is the maximum current elicited by a saturating concentration of ligand, [cGMP] is the cGMP concentration, $K_{1/2}$ is the concentration of cGMP producing half-maximal current, and h is the Hill coefficient. To confirm the formation of heteromeric CNG channels, we tested the expressed channels for block by 25 μM L-*cis*-diltiazem (Sigma-Aldrich) in the intracellular solution in the presence of 1 mM cGMP at +80 mV. For Ca^{2+}-CaM experiments, 250 nM CaM was used in intracellular solution containing 130 mM NaCl, 3 mM HEPES (pH 7.2), 2 mM nitrilotriacetic acid, and 704 mM $CaCl_2$ for a final buffered free [Ca^{2+}] of 50 μM. Niflumic acid (500 μM) was added to the pipette solution for Ca^{2+}-CaM experiments. Recordings were made at 20–22 °C. PIP_n solutions were prepared with FVPP (a phosphatase inhibitor mixture) (36) containing 5 mM sodium fluoride, 0.1 mM sodium orthovanadate, and 10 mM sodium pyrophosphate, as described previously (37). PIP_3 and PIP_2 analogues were phosphatidylinositol 3,4,5-triphosphate, dipalmitoyl, sodium salt and phosphatidylinositol 4,5-biphosphate, dipalmitoyl, and sodium salt (Matreya LLC, Pleasant Gap, PA). PIP_n solutions were applied to the cytoplasmic face of membrane patches approximately 5–10 min or more after patch excision. Data parameters were expressed as mean ± S.E. of n experiments unless indicated otherwise. Statistical significance was determined by using Student's t test or Mann-Whitney U test. $p < 0.05$ was considered statistically significant.

RESULTS

Alternative Splicing of CNGA3 Generates Channel Isoforms with Similar Fundamental Properties—Four variants of human *CNGA3* transcripts are generated by alternative splicing involving binary exclusion or inclusion of optional cassette exons 3 and 5 (24, 29). To determine the expression levels for these variants in the human retina, we designed variant-specific primers to detect the presence or absence of the optional exons (Fig. 1*A*). To confirm their specificity, we first tested these primers on plasmid cDNA representing the CNGA3 splice variants. RT quantitative PCR was used to assess the expression level of the variant *CNGA3* transcripts in human retina. We found that ~25% of retinal *CNGA3* transcripts contained exon 3, whereas more than 80% contained exon 5 (Fig. 1, *B* and *C*). Furthermore, we performed immunohistochemical studies using human retinal sections and a specific antibody targeting the exon 3-encoded sequence (Fig. 1, *D--G*). Fluorescein-coupled peanut agglutinin was used to label cone photoreceptor outer segments, the predominant location for mature cone CNG channels. We found that exon 3-containing isoforms were present in the retina and located within the outer segment of cone photoreceptors, similar to the distribution of total CNGA3 subunits detected using an antibody directed against an epitope within the C-terminal region (encoded by a constitutive exon). The observed overlap between the general CNGA3 signal and the e3-specific signal was consistent with the presence of e3 variant CNGA3 subunits in most cone photoreceptor subtypes. It is noteworthy that exon 3 appears to be unique to humans, even compared with other primates, where the related genomic sequence is not an open reading frame and the 5′ (donor) splice site does not match the consensus sequence (Fig. 2*A*).

Next, we expressed the four CNGA3 isoforms individually with CNGB3 subunits in *Xenopus* oocytes for functional analysis of the splice variants. We designated the CNGA3 isoform that lacked exon 3 but contained exon 5 as the reference CNGA3 isoform because this isoform was the first cloned and characterized (38). It is reported to be the most abundant isoform in the human retina and largely absent from other tissues (29). We found that cGMP- or cAMP-dependent activation of heteromeric CNGA3 + CNGB3 channels was not altered significantly by alternative splicing (Fig. 2, *B* and *C*). We evaluated channel activation by cGMP by measuring the concentration of cGMP that produced the half-maximal current ($K_{1/2,cGMP}$), whereas we used the ratio of maximal currents elicited by saturating concentrations of cAMP and cGMP (I_{max} cAMP/cGMP) to assess the efficacy of the partial agonist cAMP. For cone CNG channels, cGMP is nearly a full agonist, whereas cAMP is a partial agonist. For heteromeric channels containing the reference CNGA3, the $K_{1/2,cGMP}$ was 14.9 ± 0.8 μM (n = 12), and the I_{max} cAMP/cGMP was 0.26 ± 0.01 (n = 14). We found that neither the apparent cGMP affinity ($K_{1/2,cGMP}$) nor the relative cAMP efficacy (I_{max} cAMP/cGMP) of heteromeric

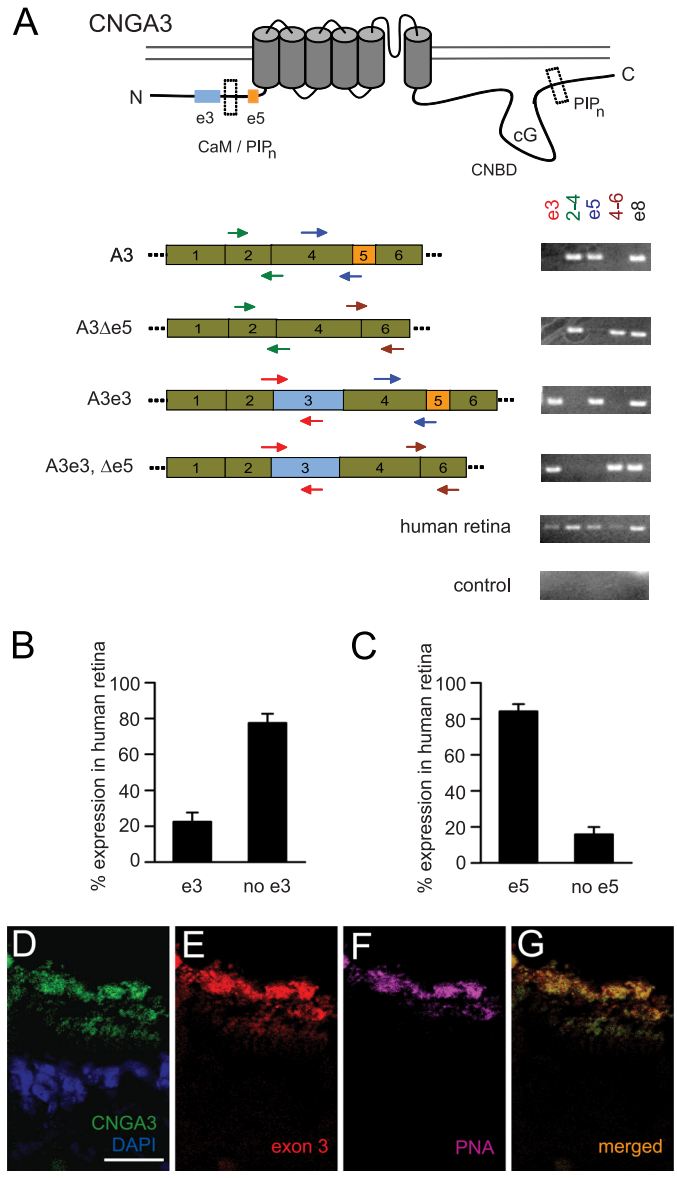

FIGURE 1. **CNGA3 splice variant-specific primers detect the relative abundance of optional exon-containing retinal transcripts.** *A*, schematic of a CNGA3 subunit (*top panel*), with regions encoded by optional exon 3 and exon 5 as well as PIP$_n$ and calmodulin regulation modules (*dashed box*) *highlighted*. Locations of PCR primer pairs for detecting inclusion or exclusion of optional exon 3 or exon 5 (note primers crossing exon boundaries) are shown *below*. Representative PCR products generated using primers sets are shown on the *left* for plasmid cDNA representing the four *CNGA3* splice variants (NM_001298, NM_001079878, AK_131300, and XM_006712243) (24, 29) and for cDNA generated from human retinal mRNA. *Control*, no template negative control; *CNBD*, cyclic nucleotide binding domain. *B* and *C*, percentage expression levels in human retinal tissue for alternative exons 3 and 5, respectively, were determined by quantitative real-time RT-PCR ($n = 3$ biological replicates with 2–3 technical replicates each). The primers used are shown in *A*. *D–G*, representative images of stained human retinal sections demonstrating the presence of CNGA3-e3 isoforms in cone outer segments. *D*, expression of total CNGA3 protein (*green*), detected using a general anti-CNGA3 antibody, with DAPI counterstaining for nuclei (*blue*). *E*, expression of the CNGA3 e3 isoform, detected using an antibody specific to the e3-encoded protein sequence (*red*). *F*, staining using the cone-specific marker peanut agglutinin (*PNA*), which labels cone outer segments (*purple*). *G*, merged image (*green* and *red*). Scale bar = 25 μm (*D–G*).

CNG channels were altered significantly by inclusion or exclusion of the optional exons (Fig. 2, *B* and *C*, $p > 0.05$ compared with channels containing the reference CNGA3). Furthermore, because there is a functionally silent Ca^{2+}-CaM binding site within the N-terminal region of CNGA3 (located within the sequence encoded by constitutive exon 4) (30), we examined the effect of alternative splicing on the Ca^{2+}-CaM sensitivity of heteromeric and homomeric channels. No differences in the Ca^{2+}-CaM sensitivity of heteromeric channels were observed with the CNGA3 splice variants (Fig. 2*D*). Application of 250 nM CaM in the presence of 50 μM free Ca^{2+} moderately attenuated the current induced by 10 μM cGMP to a similar extent for channels containing all four CNGA3 isoforms (~25% suppression). In addition, similar to reference homomeric CNGA3 channels (30), CNGA3e3-only channels remained insensitive to CaM. The current induced by 10 μM cGMP was not reduced significantly by CaM (the I_{CaM}/I ratio was 0.98 ± 0.03, $n = 6$). Together, these results indicate that alternative splicing of human CNGA3 does not modify the fundamental gating properties of the channel nor sensitivity to regulation by calmodulin. Furthermore, these results show that CNGA3 alternative splicing does not alter heteromeric channel assembly.

Alternative Splicing Tunes the Phosphoinositide Sensitivity of Heteromeric Cone CNG Channels—We tested the hypothesis that optional exon-encoded sequences might alter the phosphoinositide sensitivity of heteromeric CNGA3 + CNGB3 channels by applying diC8-PIP$_2$ or diC8-PIP$_3$ to the cytoplasmic face of the inside-out patches. Phosphoinositides were applied to patches approximately 5–10 min (or more) after patch excision. We have shown previously that application of these diC8-PIP$_n$ analogs produced similar effects on cone CNG channel gating as natural phosphoinositides (16). Also, manipulations of endogenous phosphoinositides have been shown to alter the ligand sensitivity of expressed cone CNG channels (37). We measured currents elicited by a subsaturating concentration of cGMP (5 μM), which approximates the intracellular cGMP concentration within vertebrate photoreceptors in the dark (17, 39). 10 μM PIP$_2$ suppressed the currents to a greater extent for channels formed with the optional exon 3 variant of CNGA3 (A3e3+B3) compared with channels comprised of the reference CNGA3 with CNGB3 (*A3+B3*) (Fig. 3*A*). For reference A3+B3 channels, the cGMP dose-response curve was shifted about 1.5-fold to higher concentrations of cGMP after PIP$_n$ application (Fig. 3, *B* and *C*). $K_{1/2,cGMP}$ increased from 14.3 ± 0.8 μM ($n = 14$) to 20.6 ± 1.6 μM ($n = 8$) after 1 μM diC8-PIP$_3$ (PIP$_3$) or to 22.1 ± 1.7 μM ($n = 6$) after 10 μM diC8-PIP$_2$ (PIP$_2$). Variant A3e3+B3 channels exhibited enhanced sensitivity to PIP$_n$ (Fig. 3, *B* and *C*). There was an ~2-fold greater shift in the cGMP dose-response relationship ($p < 0.001$ compared with reference channels). For A3e3+B3 channels, $K_{1/2,cGMP}$ was increased from 14.5 ± 0.9 μM ($n = 16$) to 27.1 ± 1.3 μM ($n = 10$) after 1 μM PIP$_3$ or to 32.7 ± 2.3 μM ($n = 6$) after 10 μM PIP$_2$. A similar enhancement of sensitivity to regulation by natural PIP$_2$ was observed for A3e3+B3 channels. $K_{1/2,cGMP}$ was increased from 12.5 ± 0.9 μM to 29.2 ± 2.1 μM ($n = 4$) after application of 10 μM natural PIP$_2$. Several minutes after patch excision, the contribution of endogenous PIP$_n$ to channel regulation is thought to be negligible under control conditions (37). Application of 25 μg/ml poly-lysine to control patches expressing A3+B3 channels (5–10 min after patch

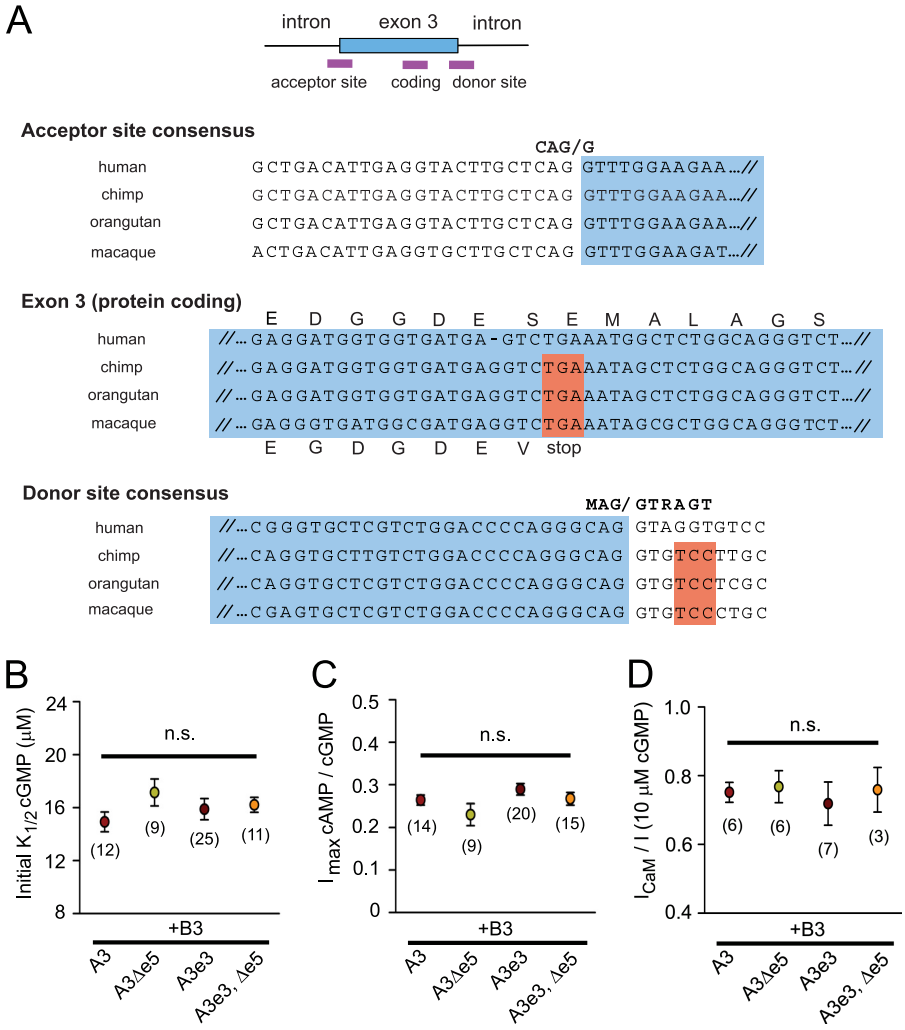

FIGURE 2. **Basic gating properties and Ca^{2+}-calmodulin sensitivity of heteromeric CNGA3+CNGB3 channels were not altered by alternative splicing of *CNGA3*.** *A*, alignment of genomic sequences for parts of human optional exon 3 and adjacent intronic sequence compared with corresponding genomic sequences of three other primates. Only human exon 3 presents an open reading frame and an intact consensus 5′ (donor) splice site. Only scant homology was apparent between human exon 3 and genomic sequences from mouse, rat, dog, cow, pig, opossum, platypus, chicken, zebrafish, *Xenopus*, and fly. Some homology was present with horse, dog, and giant panda sequences, but splice junctions were not intact (data not shown). *B*, initial apparent affinity for cGMP ($K_{1/2,cGMP}$) was not significantly different for the four human CNGA3 variants coexpressed with CNGB3 in *Xenopus* oocytes. n.s., not significantly different. *C*, relative cAMP efficacy compared with cGMP was not affected by alternative splicing of *CNGA3* transcripts. I_{max} was measured in 10 mM cAMP and 1 mM cGMP. *D*, Ca^{2+}-CaM inhibition of CNGA3+CNGB3 channels was unaffected by alternative splicing of *CNGA3* transcripts. The value below each symbol indicates the number of experiments. Data are mean ± S.E.

excision) did not increase apparent cGMP affinity. $K_{1/2,cGMP}$ was 12.7 ± 0.7 μM before and 15.7 ± 1.2 μM after poly-lysine ($p = 0.074$. $n = 4$). In contrast to the exon 3 variant, the presence or absence of exon 5-encoded sequence did not influence PIP$_n$ regulation of cone CNG channels (Fig. 3*D*). Fig. 3*E* shows the concentration-response relationship for the percent increase in $K_{1/2,cGMP}$ induced by different concentrations of PIP_2 and PIP_3 for heteromeric A3e3+B3 channels compared with A3+B3 channels. These results indicate that incorporation of the exon 3-encoded sequence significantly increased both the affinity and efficacy of PIP_2 and PIP_3 for inhibition of cGMP-dependent gating of A3+B3 channels.

The Exon 3-encoded Sequence Does Not Enhance PIP$_n$ Regulation of Homomeric CNGA3-only Channels—Homomeric CNGA3 channels are not sensitive to PIP$_n$-dependent changes in apparent cGMP affinity but, instead, show an ~2.5-fold increase in relative cAMP efficacy (I_{max} cAMP/cGMP) (16). Truncation of the C-terminal region (613X) distal to the cyclic nucleotide-binding domain, mutations disrupting the structure of the C-terminal leucine zipper domain, or charge neutralizations within the C-terminal PIP$_n$ regulation module all eliminated the increase in I_{max} cAMP/cGMP produced by PIP$_n$ for CNGA3-only channels (16, 40). We expressed the CNGA3e3 subunit without CNGB3 and found that the increase in I_{max} cAMP/cGMP after PIP$_n$ application for the homomeric channels was similar to the reference CNGA3-only channels. The fold increase in I_{max} cAMP/cGMP was 2.6 ± 0.3 ($n = 4$) after 1 μM PIP_3 or 2.2 ± 0.2 ($n = 4$) after 10 μM PIP_2. In addition, homomeric CNGA3e3 channels remained insensitive to PIP$_n$ regarding apparent cGMP affinity (Fig. 4*A*). We have shown previously that truncation of CNGA3 at amino acid 613 (CNGA3 613X) unmasks the N-terminal component of PIP$_n$ regulation for homomeric channels, producing a more than 3-fold increase in $K_{1/2,cGMP}$ after PIP$_n$ application (16). How-

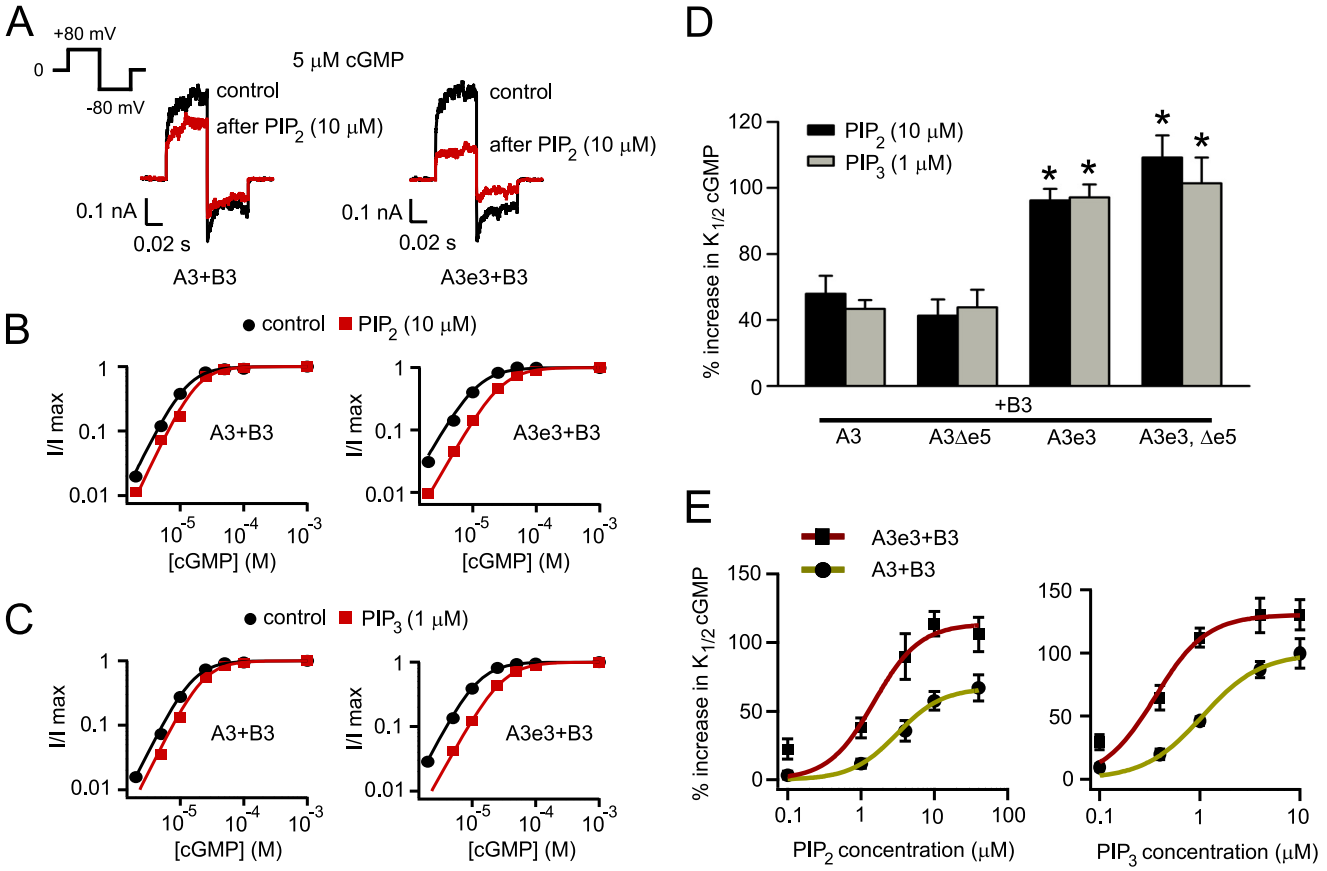

FIGURE 3. **CNGA3 optional exon 3 inclusion produces heteromeric channels with enhanced PIP$_2$ and PIP$_3$ sensitivity.** *A*, representative currents elicited by 5 μM cGMP (an approximately physiological ligand concentration) using the voltage protocol shown on the *left*, before (*black*) and after (*red*) 10 μM PIP$_2$, for heteromeric channels composed of B3 plus reference A3 or variant A3e3 expressed in *Xenopus* oocytes. The formation of heteromeric channels was confirmed by sensitivity to block by 25 μM L-*cis*-diltiazem. *B*, representative cGMP dose-response relationships for currents elicited at +80 mV before (*black*) and after (*red*) 10 μM diC8-PIP$_2$ application for activation of heteromeric A3+B3 channels, fitted using the Hill equation. Inclusion of exon e3 enhanced the rightward shift of $K_{1/2,cGMP}$ after PIP$_2$. The Hill parameters were as follows. For A3+B3 channels, before PIP$_2$, $K_{1/2,cGMP}$ = 12.9 μM, h = 2; after PIP$_2$, $K_{1/2,cGMP}$ = 18.3 μM, h = 2.1. For A3e3+B3 channels, before PIP$_2$, $K_{1/2}$ = 11.9 μM, h = 1.8; after PIP$_2$, $K_{1/2}$ = 28.0 μM, h = 1.8. *C*, representative cGMP dose-response relationships for currents elicited at +80 mV before (*black*) and after (*red*) 1 μM diC8-PIP$_3$ application for activation of heteromeric A3+B3 channels, fitted using the Hill equation. The Hill parameters were as follows. For A3+B3 channels, before PIP$_3$, $K_{1/2,cGMP}$ = 15.8 μM, h = 2; after PIP$_3$, $K_{1/2,cGMP}$ = 22.9 μM, h = 2. For A3e3+B3 channels, before PIP$_3$, $K_{1/2}$ = 12.5 μM, h = 1.9; after PIP$_3$, $K_{1/2}$ = 29.6 μM, h = 1.8. *D*, summary of the enhancement of percent increase in $K_{1/2}$ cGMP after 10 μM diC8-PIP$_2$ or 1 μM diC8-PIP$_3$ with inclusion of exon e3 but not e5. *Error bars* denote the mean ± S.E. (n = 6–16). *, $p < 0.05$ compared with channels containing the reference CNGA3 subunit, which includes exon e5. *E*, DiC8-PIP$_2$ and diC8-PIP$_3$ concentration-response relationships for the percentage of increase in $K_{1/2,cGMP}$ for activation of heteromeric A3+B3 or A3e3+B3 channels. Continuous curves represent fits using the Hill equation. The Hill parameters are as follows. For PIP$_2$, $K_{1/2}$ = 3.09 μM, h = 1.4 without e3 and $K_{1/2}$ = 1.51 μM, h = 1.4 with e3. For PIP$_3$, $K_{1/2}$ = 1.06 μM, h = 1.5 without e3 and $K_{1/2}$ = 0.36 μM, h = 1.7 with e3. *Error bars* indicate the mean ± S.E. of four independent experiments.

ever, incorporation of the region encoded by exon 3 did not significantly change the PIP$_n$-induced increase in $K_{1/2,cGMP}$ for 613X channels (Fig. 4, *A* and *B*). $K_{1/2,cGMP}$ was increased from 16.3 ± 1.0 μM (n = 11) to 64.7 ± 3.6 μM (n = 6) after 1 μM PIP$_3$ or to 53.5 ± 5.0 μM (n = 5) after 10 μM PIP$_2$ for A3e3–613X channels. These results suggest that the potentiation of PIP$_n$ sensitivity mediated by the exon 3-encoded sequence in CNGA3 requires assembly with CNGB3 subunits and/or structural elements within the distal C-terminal domain of CNGA3.

Next, we sought to determine whether the exon 3-encoded sequence was sufficient to support PIP$_n$ regulation of homomeric CNGA3 channels. To test this, we neutralized the positively charged arginines within the sequence encoded by constitutive exon 4 (R72A, R75A, R81A, R82A, and R86A in reference CNGA3; N5R-A). These changes have been shown previously to abolish the PIP$_n$ sensitivity of CNGA3–613X channels (16). We found that the PIP$_n$-induced increase in $K_{1/2,cGMP}$ of CNGA3e3–613X channels was similarly eliminated by N5R-A mutations (Fig. 4 C). This result indicated that the region encoded by alternative exon 3 alone was not sufficient to confer phosphoinositide sensitivity to homomeric CNGA3 channels. Furthermore, we carried out *in vitro* PIP$_n$-binding assays using PIP$_3$- and PIP$_2$-linked agarose beads together with GST-tagged N-terminal fragments of CNGA3 with or without the region encoded by exon 3. We found that the e3 isoform did not alter *in vitro* binding of the N-terminal fragment to PIP$_2$ or PIP$_3$ (Fig. 4*D*).

Potentiation of PIP$_n$ Sensitivity by the e3 Variant Depends on the C-terminal PIP$_n$ Regulation Module of CNGA3—PIP$_n$ regulation of heteromeric CNGA3 +CNGB3 channels is supported by two regulatory modules (N and C) (Fig. 5*A*) having additive effects on $K_{1/2,cGMP}$ (16). We silenced both N- (N5R-A) and C-terminal (R643Q and R646Q in reference CNGA3, RR-QQ) PIP$_n$ regulation modules in CNGA3e3. These mutations together have been shown previously to abolish the PIP$_n$ sensitivity of heteromeric CNGA3+CNGB3 chan-

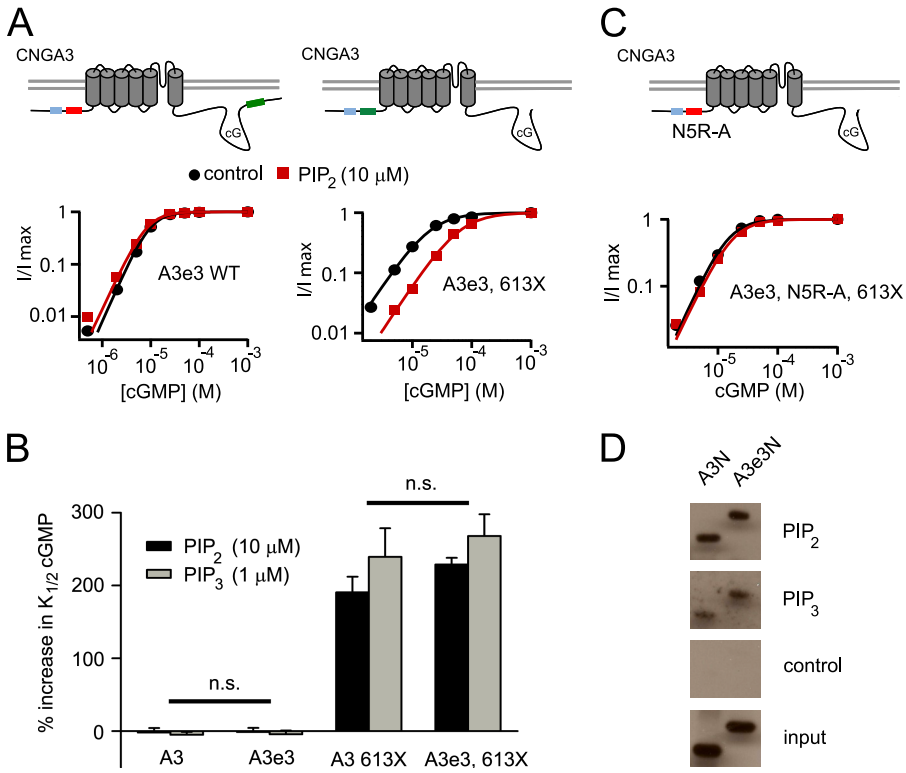

FIGURE 4. **CNGA3 exon 3 variant does not enhance PIP$_n$ regulation of homomeric CNGA3 channels nor *in vitro* PIP$_n$ binding to the N-terminal fragment.** *A*, representative cGMP dose-response relationships before and after diC8-PIP$_2$ (*red*) for activation of A3e3 wild-type or A3e3–613X channels. *Red* and *green boxes* indicate silent and active PIP$_n$ interaction sites, respectively. *Blue box*, region encoded by alternative exon 3. *cG*, cGMP. *B*, summary illustrating the impact of inclusion of exon 3 on the percentage of increase in $K_{1/2,cGMP}$ after diC8-PIP$_2$ or diC8-PIP$_3$ for homomeric wild-type A3 and A3–613X channels. Exon 3 did not produce a statistically significant effect on PIP$_n$ sensitivity for homomeric A3 channels (n = 4–6). *n.s.*, not significant. *C*, representative dose-response relationships for activation of A3e3, N5R-A, and 613X channels by cGMP. A *red box* indicates silencing of the N-terminal component for PIP$_n$ regulation of cone CNG channels by mutation (N5R-A: R72A, R75A, R81A, R82A, and R86A). *D*, *in vitro* pulldown assay using PIP$_2$, PIP$_3$, or control agarose beads combined with GST fusion proteins representing the N-terminal regions of CNGA3 either with or without the region encoded by exon 3.

nels (16). We found that channels made up of CNGA3e3-N5R-A, RR-QQ + CNGB3 subunits were no longer sensitive to PIP$_n$ (Fig. 5*B*). The percentage change in $K_{1/2,cGMP}$ was 6.3 ± 11% (n = 4) after 1 μM PIP$_3$ and −2.5 ± 5.5% (n = 6) after 10 μM PIP$_2$. This observation is consistent with the idea that the e3-encoded sequence is not sufficient to confer PIP$_n$ sensitivity to heteromeric channels. The next question we addressed was whether the enhancement of PIP$_n$ sensitivity by the e3 isoform depends on the N-, C-, or both N- and C-terminal regulatory modules. Thus, we ablated either the N-terminal or C-terminal PIP$_n$ regulation sites in CNGA3 combined with inclusion or exclusion of the region encoded by exon 3. We found that the e3 isoform still enhanced the PIP$_n$-induced increase in $K_{1/2,cGMP}$ for CNGA3+CNGB3 channels when the C-terminal PIP$_n$-regulation module was intact but the N-terminal site was silenced (N5R-A) (Fig. 5*C*, $p < 0.05$ for both PIP$_2$ and PIP$_3$). In contrast, the e3 variant was not able to potentiate the PIP$_n$-induced increase in $K_{1/2,cGMP}$ for CNGA3+CNGB3 channels when the N-terminal PIP$_n$ regulation module was intact but the C-terminal PIP$_n$ regulation module was silenced (RR-QQ) (Fig. 5*D*, p = 0.941 for PIP$_2$ and p = 0.610 for PIP$_3$). For all mutant CNGA3 subunits described here, the formation of functional heteromeric channels was confirmed by sensitivity to block by L-*cis*-diltiazem and by enhanced relative cAMP efficacy compared with homomeric channels. Therefore, these data indicate that, even though the exon 3-encoded sequence is in close proximity to the N-terminal PIP$_n$ regulation module, the CNGA3e3 variant enhances phosphoinositide sensitivity by influencing the C-terminal PIP$_n$ regulation module.

Control of PIP$_n$ Sensitivity by Alternative Splicing of Canine CNGA3—We discovered that transcripts encoding canine CNGA3 subunits also are subject to alternative splicing. There are three alternative exons encoding a region within the N-terminal cytoplasmic domain of canine CNGA3: exons 3, 4, and 5. Canine exons 3 and 4 are orthologous to human exons 4 and 5, respectively (Fig. 6*A*). Canine exon 5 has no equivalent exon in humans but is similar to exon 5 of chicken *CNGA3* (22). RT-PCR using canine retinal mRNA revealed that three splice variants of canine CNGA3 were generated: the reference canine CNGA3 with all optional exons included (cCNGA3), a variant lacking exons 3 and 4 (cCNGA3 Δe3,4), and a variant lacking exons 4 and 5 (cCNGA3Δe4,5). We tested the PIP$_n$ sensitivity of all three canine CNGA3 isoforms after expression with human CNGB3 (Fig. 6*B*). We found that channels containing cCNGA3 having a sequence encoded by all the optional exons exhibited a considerable PIP$_n$-induced increase in $K_{1/2,cGMP}$. For cCNGA3+CNGB3 channels, $K_{1/2,cGMP}$ increased from 13.9 ± 0.7 μM (n = 8) to 27.6 ± 4.0 μM (n = 4) after 1 μM PIP$_3$ or to 22.9 ± 1.8 μM (n = 4) after 10 μM PIP$_2$. Interestingly, the PIP$_n$-induced increase in $K_{1/2,cGMP}$ was eliminated for cCNGA3Δe3,4 + CNGB3 channels ($p < 0.001$ for both PIP$_2$ and PIP$_3$ compared with the reference channel). For

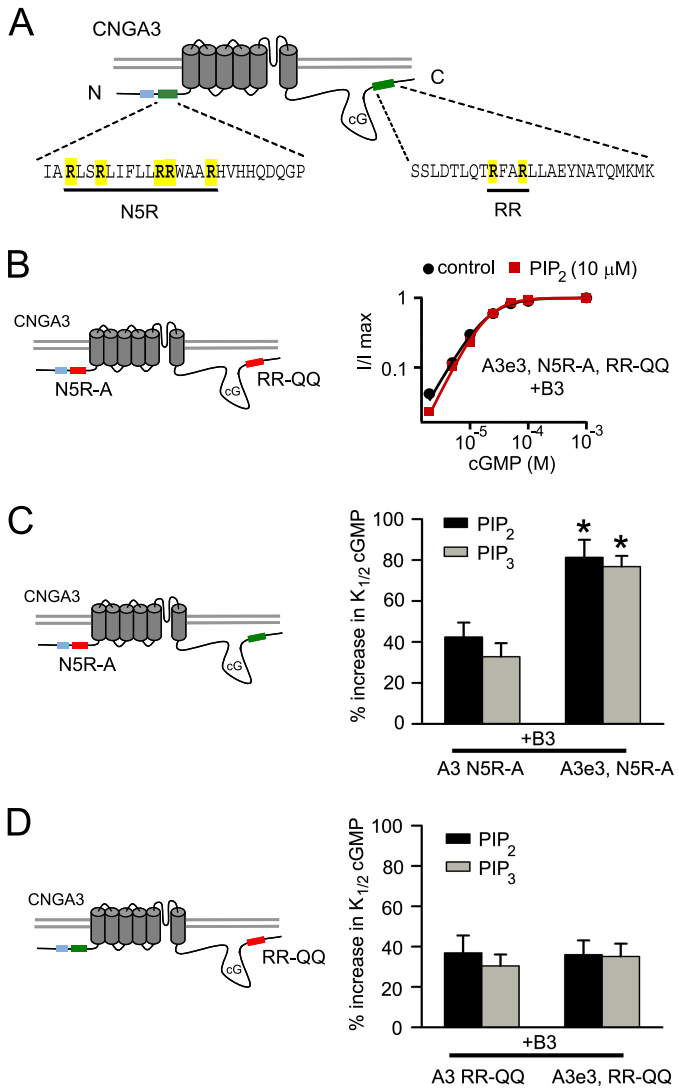

FIGURE 5. **Enhancement of PIP$_n$ sensitivity by the CNGA3 e3 isoform depends on the C-terminal structural component of PIP$_n$ regulation.** *A*, schematic illustrating the PIP$_n$ regulation modules within the N- and C-terminal regions of CNGA3, characterized by positively charged arginines (16). *B*, representative dose-response relationship for activation of heteromeric CNGA3 N5R-A, RR-QQ + B3 channels by cGMP. In this scenario, both the N-terminal (N5R-A) and C-terminal (RR-QQ: R643Q and R646Q) structural components underlying PIP$_n$ regulation were silenced by mutation. *cG*, cGMP. *C*, summary showing that the enhancement of PIP$_2$ (10 μM) or PIP$_3$ (1 μM) sensitivity by the e3 isoform was not prevented by mutation of the N-terminal PIP$_n$ regulation module (N5R-A). The *green* and *red boxes* indicate that the designated PIP$_n$ regulation module was active or silenced, respectively. *Error bars* denote the mean ± S.E. (n = 4 - 7). *, $p < 0.05$ compared with reference heteromeric channels. *D*, summary showing that mutation of residues critical for the C-terminal PIP$_n$ regulation module (RR-QQ) eliminated the enhancement of PIP$_2$ or PIP$_3$ sensitivity in $K_{1/2,cGMP}$ conferred by the e3 isoform. No significant differences were observed.

cCNGA3Δe4,5 + CNGB3 channels, the PIP$_n$-induced increase in $K_{1/2,cGMP}$ was attenuated ($p < 0.05$ for PIP$_3$). Presumably, the region encoded by exon 3 in canine *CNGA3*, similar to exon 4 in human *CNGA3*, contains a PIP$_n$ interaction site. Skipping this exon abolished the PIP$_n$ sensitivity of the channel. Together, these results indicate that alternative splicing of both canine and human *CNGA3*, with divergent splice patterns, similarly tunes the PIP$_n$ sensitivity of heteromeric cone CNG channels.

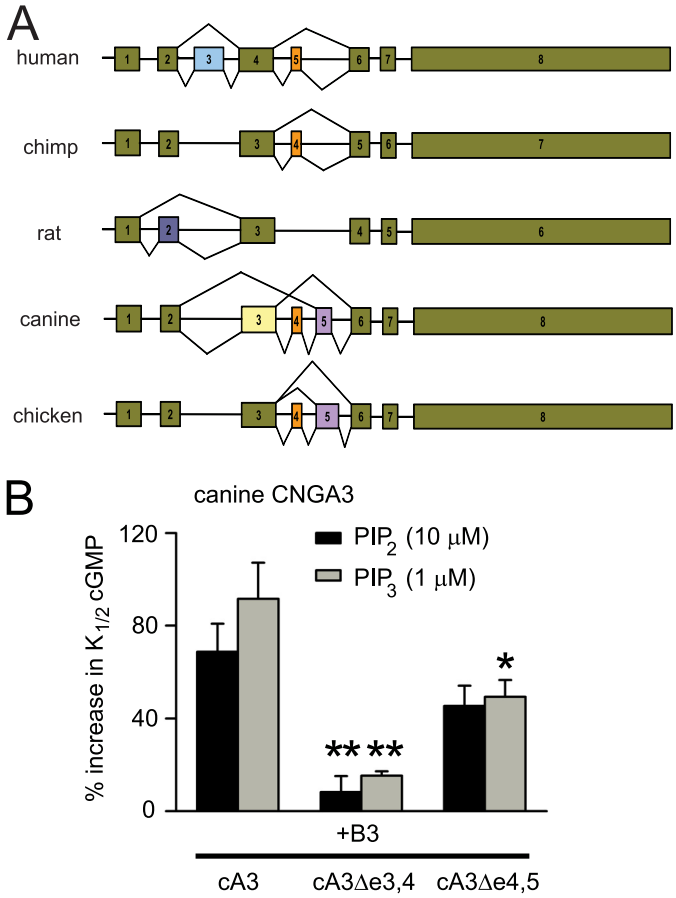

FIGURE 6. **Alternative splicing of canine *CNGA3* transcripts also tunes PIP$_n$ sensitivity.** *A*, CNGA3 splicing pattern for constitutive (*green*) and alternative cassette exons across representative species. Exon (*box*) lengths, but not intron (*line*) lengths, are shown to scale. For simplicity, removal of introns between constitutive exons is not shown. *B*, summary of PIP$_2$ and PIP$_3$ effects on $K_{1/2,cGMP}$ for heteromeric CNGA3+CNGB3 channels containing canine CNGA3 isoforms generated by alternative splicing. All subunit combinations exhibited sensitivity to blocking by L-*cis*-diltiazem, confirming the formation of functional heteromeric channels. Data are mean ± S.E. of four independent experiments. **, $p < 0.01$; *, $p < 0.05$ compared with channels having all regions encoded by e3, e4, and e5.

DISCUSSION

For genes encoding CNG channel subunits, three are known to exhibit alternatively spliced transcripts: *CNGB1*, *CNGA3*, and *CNGA1*. The functional and physiological consequences of alternative splicing of *CNGB1* have been elucidated previously (26–28, 41–43). In this work, we found that alternative splicing of *CNGA3* tunes the phosphoinositide sensitivity of cone CNG channels. Inclusion of the human-specific alternative exon 3 generated CNGA3 isoforms that significantly potentiated the PIP$_2$ or PIP$_3$ sensitivity of CNGA3+CNGB3 channels. The region encoded by exon 3 alone was not sufficient to support PIP$_n$ sensitivity in the absence of the other known PIP$_n$ regulation modules. The effect of the exon 3-encoded sequence on PIP$_n$ sensitivity appears to be mediated by an allosteric mechanism whereby the modified N-terminal cytoplasmic domain enhances the change in $K_{1/2,cGMP}$ mediated by the C-terminal PIP$_n$ regulation module of CNGA3.

Previous studies in our lab have demonstrated the importance of intersubunit N-C interactions for control of the PIP$_n$ sensitivity of cone CNG channels (16, 40). This idea is consist-

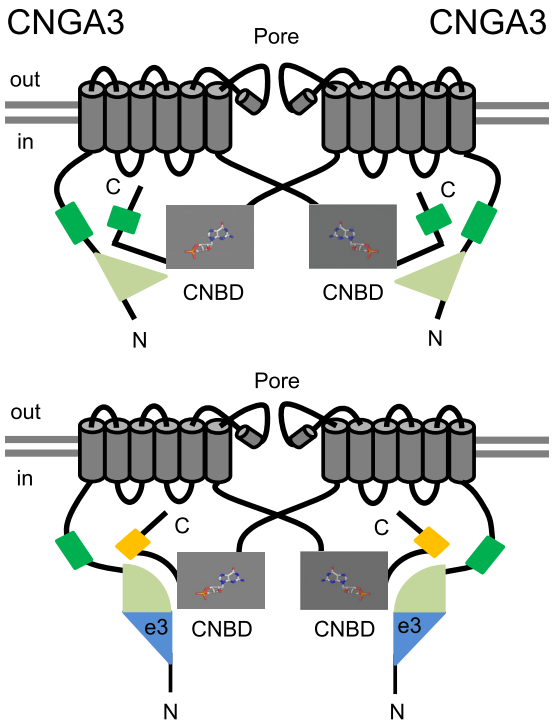

FIGURE 7. **Schematic for altered N-C coupling with the CNGA3-e3 isoform.** The model illustrates how incorporation of the e3-encoded sequence within the N-terminal region of CNGA3 may enhance the C-terminal PIP$_n$ regulation module by altering intersubunit interactions. The *green* and *yellow boxes* indicate basal and enhanced PIP$_n$ regulation modules, respectively. We propose that the interface mediating N-C coupling for CNGA3 is altered in the e3 isoform. For clarity, the CNGB3 subunits are not shown, but CNGA3-CNGB3 interactions may also be altered for channels containing the e3 isoform. *CNBD*, cyclic nucleotide binding domain.

ent with the results described here for enhancement of PIP$_n$ sensitivity by exon 3 inclusion, which inserts 55 additional amino acids into the N-terminal domain but depends on the C-terminal PIP$_n$ regulation module rather than the adjacent N-terminal PIP$_n$ regulation site. Although the exact mechanism underlying potentiation of PIP$_n$ sensitivity in the e3 isoform is not fully understood, we hypothesize that, with the assistance of CNGB3, the conformational difference in the CNGA3 N-terminal region caused by inclusion or exclusion of the region encoded by exon 3 is coupled to the C-terminal region of the adjacent CNGA3 subunit, altering the ability of the C-terminal PIP$_n$ regulation module to respond to membrane-bound phosphoinositides (Fig. 7). In other words, incorporation of the exon 3-encoded sequence modulates the N-C interactions of CNGA3 subunits, thus potentiating the PIP$_n$ sensitivity of cone CNG channels. The exon 3-encoded sequence may also influence CNGA3-CNGB3 interactions because these are also thought to modulate PIP$_n$ sensitivity and the competency of the C-terminal PIP$_n$ regulation module in CNGA3 to confer a change in $K_{1/2,cGMP}$ (16). Interestingly, in addition to well characterized N-C-terminal interactions for CNG channels (32, 44–47, 28), a recent crystal structure of the EAG domain-cyclic nucleotide-binding homology domain (CNBHD) complex of homologous mEAG1 (KCNH) channels revealed that the post-CNBHD region (equivalent to the region adjacent to the C-terminal PIP$_n$ regulation module in CNGA3) is interacting directly with the N-terminal EAG domain (48). Moreover, we have shown previously that truncations and point mutations in this post-cyclic nucleotide-binding domain region can influence the N-terminal PIP$_n$ regulation module of CNGA3 (16, 40). We propose that the coupling between N- and C-terminal regions of CNGA3 (and presumably CNGB3) is an essential element of cone CNG channel regulation. However, more sophisticated structural approaches may be required to elucidate the precise interdomain contacts and detailed conformational changes associated with the e3 variant.

We found that alternative splicing of canine *CNGA3* also regulates the phosphoinositide sensitivity of the resulting channels. Together, these findings suggest that the functional significance of *CNGA3* alternative splicing might be conserved across species, despite the divergence in exon combinations for the orthologous genes. Considering that exon 3-containing transcripts were expressed in 23 human tissues, including heart, kidney, and brain (29), enhanced phosphoinositide sensitivity by CNGA3e3 may have widespread physiological significance. However, how tuning of PIP$_n$ regulation of CNG channels by alternative splicing is related to function in cone photoreceptors and other cell types is not understood. The functional importance of optional exon 5 remains elusive. On the basis of previous work showing that the human *CNGA3* e5-containing transcripts were expressed primarily in the retina (29), exon 5 might contain features favoring its inclusion here, such as exonic splicing enhancers recognized by neuron- or retina-specific splicing factors expressed in a tissue-specific manner. The splicing factors and *cis*-regulatory features driving e3 inclusion also are unknown. The sequence upstream of exon 3 presents a weak poly-pyrimidine tract that likely necessitates splicing enhancer sequences that facilitate e3 inclusion.

The functional CNGA3e3 variant seems to represent a recent innovation along the human evolutionary pathway. Comparative analysis of alternative splicing patterns in humans and chimpanzees reveal that, for at least 4% of genes, one or more cassette alternative exons display pronounced splicing differences between the species (49). Human-specific patterns of alternative splicing have been found to be particularly widespread within the brain (50). Also, it has been estimated that humans and chimpanzees differ by at least 6% in their complement of genes (51). The trichromatic visual system is one of the dramatic specializations present in the human lineage compared with other mammals. It is not entirely surprising that unique patterns of splicing and/or gene regulation may be related to these specializations (52, 53).

Acknowledgments—We thank Elizabeth Rich for technical support; Changhong Peng, Daylene Mills, and Tealia Davis for performing pilot studies; King-Wai Yau for sharing the cDNA clone for human CNGA3; and Peter Meighan and Lane Brown for constructive input.

REFERENCES

1. Burns, M. E., and Arshavsky, V. Y. (2005) Beyond counting photons: trials and trends in vertebrate visual transduction. *Neuron* **48,** 387–401
2. Jan, L. Y., and Jan, Y. N. (1990) A superfamily of ion channels. *Nature* **345,** 672
3. Isacoff, E. Y., Jan, L. Y., and Minor, D. L., Jr. (2013) Conduits of life's spark: a perspective on ion channel research since the birth of neuron. *Neuron*

80, 658–674
4. Craven, K. B., and Zagotta, W. N. (2006) CNG and HCN channels: two peas, one pod. *Annu. Rev. Physiol.* **68,** 375–401
5. Hsu, Y. T., and Molday, R. S. (1993) Modulation of the cGMP-gated channel of rod photoreceptor cells by calmodulin. *Nature* **361,** 76–79
6. Gordon, S. E., Downing-Park, J., and Zimmerman, A. L. (1995) Modulation of the cGMP-gated ion channel in frog rods by calmodulin and an endogenous inhibitory factor. *J. Physiol.* **486,** 533–546
7. Trudeau, M. C., and Zagotta, W. N. (2003) Calcium/calmodulin modulation of olfactory and rod cyclic nucleotide-gated ion channels. *J. Biol. Chem.* **278,** 18705–18708
8. Trudeau, M. C., and Zagotta, W. N. (2004) Dynamics of Ca^{2+}-calmodulin-dependent inhibition of rod cyclic nucleotide-gated channels measured by patch-clamp fluorometry. *J. Gen. Physiol.* **124,** 211–223
9. Bradley, J., Bönigk, W., Yau, K.-W., and Frings, S. (2004) Calmodulin permanently associates with rat olfactory CNG channels under native conditions. *Nat. Neurosci.* **7,** 705–710
10. Molokanova, E., Maddox, F., Luetje, C. W., and Kramer, R. H. (1999) Activity-dependent modulation of rod photoreceptor cyclic nucleotide-gated channels mediated by phosphorylation of a specific tyrosine residue. *J. Neurosci.* **19,** 4786–4795
11. Gordon, S. E., Brautigan, D. L., and Zimmerman, A. L. (1992) Protein phosphatases modulate the apparent agonist affinity of the light-regulated ion channel in retinal rods. *Neuron* **9,** 739–748
12. Meighan, P. C., Meighan, S. E., Rich, E. D., Brown, R. L., and Varnum, M. D. (2012) Matrix metalloproteinase-9 and -2 enhance the ligand sensitivity of photoreceptor cyclic nucleotide-gated channels. *Channels Austin* **6,** 181–196
13. Meighan, S. E., Meighan, P. C., Rich, E. D., Brown, R. L., and Varnum, M. D. (2013) Cyclic nucleotide-gated channel subunit glycosylation regulates matrix metalloproteinase-dependent changes in channel gating. *Biochemistry* **52,** 8352–8362
14. Womack, K. B., Gordon, S. E., He, F., Wensel, T. G., Lu, C. C., and Hilgemann, D. W. (2000) Do phosphatidylinositides modulate vertebrate phototransduction? *J. Neurosci.* **20,** 2792–2799
15. Brady, J. D., Rich, E. D., Martens, J. R., Karpen, J. W., Varnum, M. D., and Brown, R. L. (2006) Interplay between PIP3 and calmodulin regulation of olfactory cyclic nucleotide-gated channels. *Proc. Natl. Acad. Sci. U.S.A.* **103,** 15635–15640
16. Dai, G., Peng, C., Liu, C., and Varnum, M. D. (2013) Two structural components in CNGA3 support regulation of cone CNG channels by phosphoinositides. *J. Gen. Physiol.* **141,** 413–430
17. Fain, G. L., Matthews, H. R., Cornwall, M. C., and Koutalos, Y. (2001) Adaptation in vertebrate photoreceptors. *Physiol. Rev.* **81,** 117–151
18. Ko, G. Y., Ko, M. L., and Dryer, S. E. (2004) Circadian regulation of cGMP-gated channels of vertebrate cone photoreceptors: role of cAMP and Ras. *J. Neurosci.* **24,** 1296–1304
19. Chen, S.-K., Ko, G. Y., and Dryer, S. E. (2007) Somatostatin peptides produce multiple effects on gating properties of native cone photoreceptor cGMP-gated channels that depend on circadian phase and previous illumination. *J. Neurosci.* **27,** 12168–12175
20. Körschen, H. G., Illing, M., Seifert, R., Sesti, F., Williams, A., Gotzes, S., Colville, C., Müller, F., Dosé, A., and Godde, M. (1995) A 240 kDa protein represents the complete β subunit of the cyclic nucleotide-gated channel from rod photoreceptor. *Neuron* **15,** 627–636
21. Sautter, A., Zong, X., Hofmann, F., and Biel, M. (1998) An isoform of the rod photoreceptor cyclic nucleotide-gated channel β subunit expressed in olfactory neurons. *Proc. Natl. Acad. Sci. U.S.A.* **95,** 4696–4701
22. Bönigk, W., Müller, F., Middendorff, R., Weyand, I., and Kaupp, U. B. (1996) Two alternatively spliced forms of the cGMP-gated channel α-subunit from cone photoreceptor are expressed in the chick pineal organ. *J. Neurosci.* **16,** 7458–7468
23. Meyer, M. R., Angele, A., Kremmer, E., Kaupp, U. B., and Muller, F. (2000) A cGMP-signaling pathway in a subset of olfactory sensory neurons. *Proc. Natl. Acad. Sci. U.S.A.* **97,** 10595–10600
24. Wissinger, B., Gamer, D., Jägle, H., Giorda, R., Marx, T., Mayer, S., Tippmann, S., Broghammer, M., Jurklies, B., Rosenberg, T., Jacobson, S. G., Sener, E. C., Tatlipinar, S., Hoyng, C. B., Castellan, C., Bitoun, P., Andreasson, S., Rudolph, G., Kellner, U., Lorenz, B., Wolff, G., Verellen-Dumoulin, C., Schwartz, M., Cremers, F. P., Apfelstedt-Sylla, E., Zrenner, E., Salati, R., Sharpe, L. T., and Kohl, S. (2001) CNGA3 mutations in hereditary cone photoreceptor disorders. *Am. J. Hum. Genet.* **69,** 722–737
25. Blencowe, B. J. (2006) Alternative splicing: new insights from global analyses. *Cell* **126,** 37–47
26. Körschen, H. G., Beyermann, M., Müller, F., Heck, M., Vantler, M., Koch, K. W., Kellner, R., Wolfrum, U., Bode, C., Hofmann, K. P., and Kaupp, U. B. (1999) Interaction of glutamic-acid-rich proteins with the cGMP signalling pathway in rod photoreceptors. *Nature* **400,** 761–766
27. Poetsch, A., Molday, L. L., and Molday, R. S. (2001) The cGMP-gated channel and related glutamic acid-rich proteins interact with peripherin-2 at the rim region of rod photoreceptor disc membranes. *J. Biol. Chem.* **276,** 48009–48016
28. Michalakis, S., Zong, X., Becirovic, E., Hammelmann, V., Wein, T., Wanner, K. T., and Biel, M. (2011) The glutamic acid-rich protein is a gating inhibitor of cyclic nucleotide-gated channels. *J. Neurosci.* **31,** 133–141
29. Cassar, S. C., Chen, J., Zhang, D., and Gopalakrishnan, M. (2004) Tissue specific expression of alternative splice forms of human cyclic nucleotide gated channel subunit CNGA3. *Mol. Vis.* **10,** 808–813
30. Grunwald, M. E., Zhong, H., Lai, J., and Yau, K. W. (1999) Molecular determinants of the modulation of cyclic nucleotide-activated channels by calmodulin. *Proc. Natl. Acad. Sci. U.S.A.* **96,** 13444–13449
31. Weitz, D., Zoche, M., Müller, F., Beyermann, M., Körschen, H. G., Kaupp, U. B., and Koch, K. W. (1998) Calmodulin controls the rod photoreceptor CNG channel through an unconventional binding site in the N-terminus of the β-subunit. *EMBO J.* **17,** 2273–2284
32. Varnum, M. D., and Zagotta, W. N. (1997) Interdomain interactions underlying activation of cyclic nucleotide-gated channels. *Science* **278,** 110–113
33. Michalakis, S., Geiger, H., Haverkamp, S., Hofmann, F., Gerstner, A., and Biel, M. (2005) Impaired opsin targeting and cone photoreceptor migration in the retina of mice lacking the cyclic nucleotide-gated channel CNGA3. *Invest. Ophthalmol. Vis. Sci.* **46,** 1516–1524
34. Varnum, M. D., Black, K. D., and Zagotta, W. N. (1995) Molecular mechanism for ligand discrimination of cyclic nucleotide-gated channels. *Neuron* **15,** 619–625
35. Peng, C., Rich, E. D., and Varnum, M. D. (2004) Subunit configuration of heteromeric cone cyclic nucleotide-gated channels. *Neuron* **42,** 401–410
36. Huang, C. L., Feng, S., and Hilgemann, D. W. (1998) Direct activation of inward rectifier potassium channels by PIP2 and its stabilization by G$\beta\gamma$. *Nature* **391,** 803–806
37. Bright, S. R., Rich, E. D., and Varnum, M. D. (2007) Regulation of human cone cyclic nucleotide-gated channels by endogenous phospholipids and exogenously applied phosphatidylinositol 3,4,5-trisphosphate. *Mol. Pharmacol.* **71,** 176–183
38. Yu, W. P., Grunwald, M. E., and Yau, K. W. (1996) Molecular cloning, functional expression and chromosomal localization of a human homolog of the cyclic nucleotide-gated ion channel of retinal cone photoreceptors. *FEBS Lett.* **393,** 211–215
39. Pugh, E. N., Jr., Nikonov, S., and Lamb, T. D. (1999) Molecular mechanisms of vertebrate photoreceptor light adaptation. *Curr. Opin. Neurobiol.* **9,** 410–418
40. Dai, G., and Varnum, M. D. (2013) CNGA3 achromatopsia-associated mutation potentiates the phosphoinositide sensitivity of cone photoreceptor CNG channels by altering intersubunit interactions. *Am. J. Physiol. Cell Physiol.* **305,** C147–C159
41. Haber-Pohlmeier, S., Abarca-Heidemann, K., Körschen, H. G., Dhiman, H. K., Heberle, J., Schwalbe, H., Klein-Seetharaman, J., Kaupp, U. B., and Pohlmeier, A. (2007) Binding of Ca^{2+} to glutamic acid-rich polypeptides from the rod outer segment. *Biophys. J.* **92,** 3207–3214
42. Zhang, Y., Molday, L. L., Molday, R. S., Sarfare, S. S., Woodruff, M. L., Fain, G. L., Kraft, T. W., and Pittler, S. J. (2009) Knockout of GARPs and the β-subunit of the rod cGMP-gated channel disrupts disk morphogenesis and rod outer segment structural integrity. *J. Cell Sci.* **122,** 1192–1200
43. Ritter, L. M., Khattree, N., Tam, B., Moritz, O. L., Schmitz, F., and Goldberg, A. F. (2011) *In situ* visualization of protein interactions in sensory neurons: glutamic acid-rich proteins (GARPs) play differential roles for

photoreceptor outer segment scaffolding. *J. Neurosci.* **31,** 11231–11243
44. Gordon, S. E., Varnum, M. D., and Zagotta, W. N. (1997) Direct interaction between amino- and carboxyl-terminal domains of cyclic nucleotide-gated channels. *Neuron* **19,** 431–441
45. Trudeau, M. C., and Zagotta, W. N. (2002) Mechanism of calcium/calmodulin inhibition of rod cyclic nucleotide-gated channels. *Proc. Natl. Acad. Sci. U.S.A.* **99,** 8424–8429
46. Trudeau, M. C., and Zagotta, W. N. (2002) An intersubunit interaction regulates trafficking of rod cyclic nucleotide-gated channels and is disrupted in an inherited form of blindness. *Neuron* **34,** 197–207
47. Zheng, J., Varnum, M. D., and Zagotta, W. N. (2003) Disruption of an intersubunit interaction underlies Ca^{2+}-calmodulin modulation of cyclic nucleotide-gated channels. *J. Neurosci.* **23,** 8167–8175
48. Haitin, Y., Carlson, A. E., and Zagotta, W. N. (2013) The structural mechanism of KCNH-channel regulation by the EAG domain. *Nature* **501,** 444–448
49. Calarco, J. A., Xing, Y., Cáceres, M., Calarco, J. P., Xiao, X., Pan, Q., Lee, C., Preuss, T. M., and Blencowe, B. J. (2007) Global analysis of alternative splicing differences between humans and chimpanzees. *Genes Dev.* **21,** 2963–2975
50. Lin, L., Shen, S., Jiang, P., Sato, S., Davidson, B. L., and Xing, Y. (2010) Evolution of alternative splicing in primate brain transcriptomes. *Hum. Mol. Genet.* **19,** 2958–2973
51. Demuth, J. P., De Bie, T., Stajich, J. E., Cristianini, N., and Hahn, M. W. (2006) The evolution of mammalian gene families. *PloS ONE* **1,** e85
52. Ward, L. D., and Kellis, M. (2012) Evidence of abundant purifying selection in humans for recently acquired regulatory functions. *Science* **337,** 1675–1678
53. Farkas, M. H., Grant, G. R., White, J. A., Sousa, M. E., Consugar, M. B., and Pierce, E. A. (2013) Transcriptome analyses of the human retina identify unprecedented transcript diversity and 3.5 Mb of novel transcribed sequence via significant alternative splicing and novel genes. *BMC Genomics* **14,** 486